Available online at www.sciencedirect.com
ScienceDirect
PHOTONICS AND NANOSTRUCTURES Fundamentals and Applications
Photonics and Nanostructures – Fundamentals and Applications 10 (2012) 276–280
www.elsevier.com/locate/photonics

Loss compensated negative index material at optical wavelengths

Anan Fang [a,*], Zhixiang Huang [a,b], Thomas Koschny [a,c], Costas M. Soukoulis [a,c]

[a] Department of Physics and Astronomy and Ames Laboratory, Iowa State University, Ames, IA 50011, USA
[b] Key Laboratory of Intelligent Computing and Signal Processing, Anhui University, Hefei 230039, China
[c] Department of Materials Science and Technology and Institute of Electronic Structure and Laser, FORTH, University of Crete, 71110 Heraklion, Crete, Greece

Received 6 January 2011; received in revised form 3 May 2011; accepted 12 May 2011
Available online 20 May 2011

Abstract: We present a computational approach, allowing for a self-consistent treatment of three-dimensional (3D) fishnet metamaterial operating at 710 nm wavelength coupled to a gain material incorporated into the nanostructure. We show numerically that loss-free negative index material is achievable by incorporating gain material inside the fishnet structure. The effective gain coefficient of the combined fishnet-gain system is much larger than its bulk counterpart and the figure-of-merit (FOM = | Re(n)/ Im(n) |) increases dramatically with gain. Transmission, reflection, and absorption data, as well as the retrieved effective parameters, are presented for the fishnet structure with and without gain.
Published by Elsevier B.V.

Keywords: Fishnet metamaterial; Gain materials; Loss compensation; Magnetic resonance

1. Introduction

The field of metamaterials has seen spectacular experimental progress in recent years [1–7]. However, the intrinsic metallic Joule losses in the metal-based structures hinder the development of metamaterials for almost all the applications at optical wavelengths. Generally, losses are orders of magnitude too large for the envisioned applications, such as, perfect lenses [8], and invisibility cloaking [9]. So, reducing the losses becomes extremely important and necessary. However, achieving such reduction of losses by geometric tailoring of the metamaterial designs [10–13] appears to be out of reach. Thus, as a generic way, incorporation of gain material has to be studied systematically. One important issue is not to assume the metamaterial structure and the gain medium are independent from one another [14–20]. In fact, increasing the gain in the metamaterial changes the metamaterial properties, which, in turn, changes the coupling to the gain medium until a steady state is reached. So, there is a need for self-consistent calculations [21–25] for incorporating gain materials into realistic metamaterials.

Parametric self-consistent calculations of gain incorporated into 2D magnetic metamaterials [22,23] and 3D realistic fishnet structures [24,25] have been recently reported. Results have shown introducing the gain might promise remedy on the loss issue of metamaterials. It is demonstrated the effective gain coefficient of the combined system can be much higher than its bulk counterpart due to the strong local-field enhancement inside the metamaterial designs [26–28,22]. Recently some experiments on gain have been done using quantum dots [29], single quantum wells [30] or organic dyes [31]. In Refs. [29,30], only part of the loss was compensated in experiments, and the metamaterial structures do not have negative n. So far, to the best of our knowledge, the experimental

* Corresponding author. Tel.: +1 515 294 3985.
E-mail address: aafang@iastate.edu (A. Fang).

1569-4410/$ – see front matter. Published by Elsevier B.V.
doi:10.1016/j.photonics.2011.05.003

realization of the loss-free negative index material with gain was only reported by Xiao et al. [31]. They embedded the epoxy doped with Rh800 dye molecules into a silver fishnet structure operating at around 0.7 μm (red light) wavelength and observed a relative transmittance enhancement in the order of 100% with optical pump. By comparison with numerical calculations they claimed the losses were fully compensated by gain at a certain wavelength range.

In this paper, we apply a detailed time-domain self-consistent computational model on a fishnet metamaterial also operating at red light with gain. It is found the gain can compensate the losses of the fishnet structure and the transmission, reflection and absorption spectra with gain show a strong resonant behavior due to the loss compensation.

2. Theoretical model

Instead of simply forcing negative imaginary part of the gain material response function such that produces unrealistic linear gain, the gain in our model is described by a generic four-level atomic system, which tracks fields and occupation numbers at each point in space, taking into account energy exchange between atoms and fields, electronic pumping, and non-radiative decays [32]. An external mechanism pumps electrons from the ground state level, N_0, to the third level, N_3, at a certain pumping rate, Γ_{pump}, proportional to the optical pumping intensity in an experiment. After a short lifetime, τ_{32}, electrons transfer non-radiatively into the metastable second level, N_2. The second level (N_2) and the first level (N_1) are called the upper and lower lasing levels. Electrons can be transferred from the upper to the lower lasing level by spontaneous and stimulated emissions. At last, electrons transfer quickly and non-radiatively from the first level (N_1) to the ground state level (N_0). The lifetimes and energies of the upper and lower lasing levels are τ_{21}, E_2 and τ_{10}, E_1, respectively. The center frequency of the radiation is $\omega_a = (E_2 - E_1)/\hbar$, chosen to have $\lambda_a = 2\pi/\omega_a = 710$ nm. The parameters, τ_{32}, τ_{21}, and τ_{10}, are chosen 1.0×10^{-13}, 5.0×10^{-10}, and 1.0×10^{-13} s, respectively. The total electron density, $N_0(t=0) = N_0(t) + N_1(t) + N_2(t) + N_3(t) = 6.0 \times 10^{24}/\text{m}^3$, and the pumping rate, Γ_{pump}, is an external parameter. These gain parameters are taken from Rh800 dye molecules [33]. The time-dependent Maxwell equations are given by $\nabla \times \mathbf{E} = -\partial \mathbf{B}/\partial t$ and $\nabla \times \mathbf{H} = \varepsilon\varepsilon_o \partial \mathbf{E}/\partial t + \partial \mathbf{P}/\partial t$, where $\mathbf{B} = \mu\mu_o\mathbf{H}$ and $\mathbf{P}$ is the dispersive electric polarization density from which the amplification and gain can be obtained. Following the single electron case, we can show [32] the polarization density $\mathbf{P}(\mathbf{r}, t)$ in the presence of an electric field obeys locally the following equation of motion,

$$\frac{\partial^2 \mathbf{P}(t)}{\partial t^2} + \Gamma_a \frac{\partial \mathbf{P}(t)}{\partial t} + \omega_a^2 \mathbf{P}(t) = -\sigma_a \Delta N(t) \mathbf{E}(t), \tag{1}$$

where Γ_a is the linewidth of the atomic transition ω_a and is equal to 10^{14} rad/s [33]. The factor, $\Delta N(\mathbf{r}, t) = N_2(\mathbf{r}, t) - N_1(\mathbf{r}, t)$, is the population inversion that drives the polarization, and σ_a is the coupling strength of $\mathbf{P}$ to the external electric field and its value is taken to be 5×10^{-7} C^2/kg. It follows [32] from Eq. (1) that the amplification line shape is Lorentzian and homogeneously broadened. The occupation numbers at each spatial point vary according to

$$\frac{\partial N_3}{\partial t} = \Gamma_{\text{pump}} N_0 - \frac{N_3}{\tau_{32}}, \tag{2a}$$

$$\frac{\partial N_2}{\partial t} = \frac{N_3}{\tau_{32}} + \frac{1}{\hbar\omega_a} \mathbf{E} \cdot \frac{\partial \mathbf{P}}{\partial t} - \frac{N_2}{\tau_{21}}, \tag{2b}$$

$$\frac{\partial N_1}{\partial t} = \frac{N_2}{\tau_{21}} - \frac{1}{\hbar\omega_a} \mathbf{E} \cdot \frac{\partial \mathbf{P}}{\partial t} - \frac{N_1}{\tau_{10}}, \tag{2c}$$

$$\frac{\partial N_0}{\partial t} = \frac{N_1}{\tau_{10}} - \Gamma_{\text{pump}} N_0, \tag{2d}$$

where $(1/\hbar\omega_a)\mathbf{E} \cdot (\partial \mathbf{P}/\partial t)$ is the induced radiation rate or excitation rate depending on its sign.

To solve the behavior of the gain materials in the electromagnetic fields numerically, the finite-difference time-domain (FDTD) technique is utilized [34]. In the FDTD calculations, the discrete time and space steps are chosen to be $\Delta t = 8.0 \times 10^{-18}$ s and $\Delta x = 5 \times 10^{-9}$ m. The initial condition is that all the electrons are in the ground state and all electric, magnetic and polarization fields are zero. Then, the electrons are pumped from N_0 to N_3 (then relaxing to N_2) with a constant pumping rate, Γ_{pump}. The system begins to evolve according to the system of equations above.

3. Numerical calculations

The unit cell of the fishnet structure in simulations is shown in Fig. 1. The structure is perforated and the dielectric in the hole is set as vacuum. The size of the unit cell along the propagation direction is $h = 2h_m + h_s + 2h_d$, where h_m, h_s and h_d are the thicknesses of the metal layer, the spacer and the dielectric layer on the top/bottom surface, respectively. Consider two configurations, one without gain and one with gain. For the configuration with gain, two thin dielectric layers of thickness, $(h_s - h_g)/2$, are introduced to separate the gain from

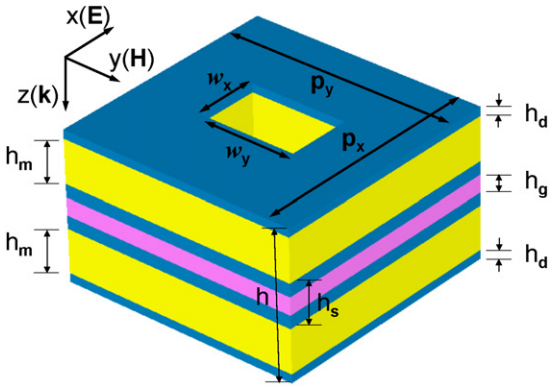

Fig. 1. Unit cell of the perforated fishnet structure with gain embedded in-between two metal (silver) layers. The geometric parameters are $p_x = p_y = 280$ nm, $w_x = 75$ nm, $w_y = 115$ nm, $h = 170$ nm, $h_m = h_s = 50$ nm, $h_d = 10$ nm and $h_g = 20$ nm. The thicknesses of the silver (yellow) and gain (magenta) layer are h_m and h_g, respectively. The dielectric layer (blue) and the gain have a refractive index $n = 1.65$. (For interpretation of the references to color in this figure legend, the reader is referred to the web version of the article.)

the metal layers so that the quenching effect can be avoided. The thickness of the gain layer is h_g. The emission wavelength of the gain is 710 nm. The full width at half maximum (FWHM) of the gain is 26.8 nm. To account for the additional loss due to the electron scattering in the nanostructure, we increase the loss of silver by a factor of 3 relative to its bulk counterpart. Notice the propagation direction is perpendicular to the fishnet plane with the electric and magnetic fields along the x and y directions, respectively. All the dimensions are chosen such that the magnetic resonance of the fishnet structure has a resonance wavelength $\lambda_R = 710$ nm, which overlaps with the peak of the emission of the gain material.

We start the calculations without gain, then increase the pumping rate, Γ_{pump} from 0 to 3.0×10^8 s^{-1}. In Fig. 2, we plot the transmission, T, (2a), reflection, R, (2b), and absorption, $A = 1 - T - R$, (2c) as a function of wavelength for different pumping rates. Notice the wavelength dependence of T and R for different pumping rates away from the resonance wavelength, $\lambda_R = 710$ nm, are the same. Around the resonance wavelength, the transmission, T, has a peak and increases with the pumping rate. The reflection, R, shows a dip around the resonance wavelength, which gets deeper and narrower as the pumping rate increases. Notice in Fig. 2(a), T without gain is very weak. However, with the introduction of gain, the transmission gets much larger and clearly shows a resonant behavior. The absorption, A, is plotted in Fig. 2(c) as a function of wavelength for different pumping rates. We notice the absorption peak gets narrower as the pumping rate increases because the gain undamps the resonance. The absorption first increases at the resonance wavelength with the pumping rate because the gain changes the impedance of the fishnet metamaterial and more electromagnetic energy goes through the sample. As the gain further increases, the absorption decreases and finally at the pumping rate of 3.0×10^8 s^{-1}, it becomes negative, i.e., the gain overcompensates the losses. So the gain can compensate the losses of the fishnet structure.

In addition, we plot the retrieved results of the real and imaginary parts of the magnetic permeability, μ, with and without gain in Fig. 3(a) by inverting the scattering amplitudes [35,36]. Without gain, the magnetic permeability μ is very flat and we almost can not see the existence of a resonance because the large loss damps the magnetic resonance. As gain increases, the Re(μ) becomes sharper around the resonance wavelength and the Im(μ) becomes much narrower since the gain compensates the losses and hence the resonance is undamped. The negative permittivity mainly comes from the continuous metallic wires. However, the dipole interaction between the corresponding electric dipole and gain material is dominated by the propagation field $O(\omega \ln |kr|)$, and very weak, such that both the real and imaginary parts of

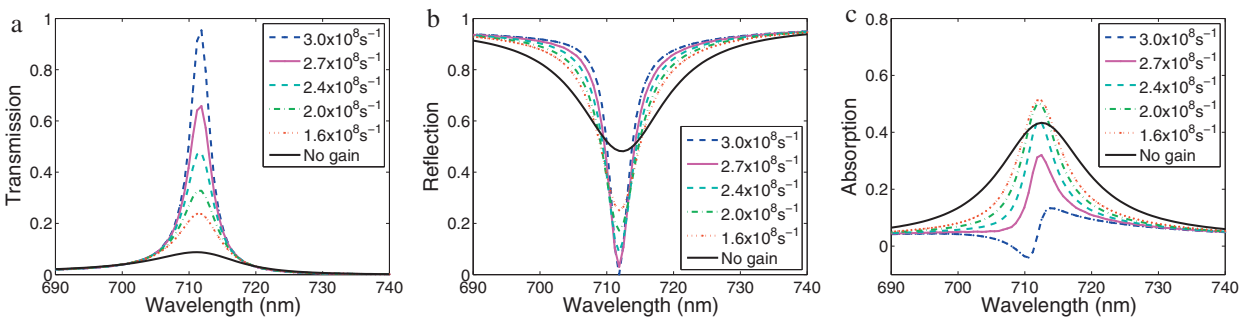

Fig. 2. The transmission (a), reflection (b) and absorption (c) as a function of wavelength for different pumping rates.

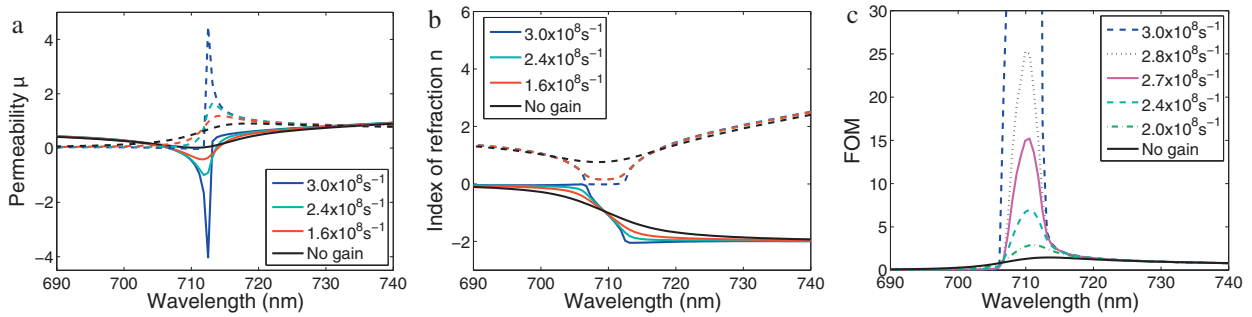

Fig. 3. The retrieved results for the real (solid lines) and the imaginary (dashed lines) parts of (a) the effective permeability, μ, and (b) the corresponding effective index of refraction, n, without and with gain for different pumping rates. (c) The figure-of-merit (FOM) as a function of wavelength for different pumping rates.

the effective permittivity almost do not change with the introduction of gain. In Fig. 3(b), we plot the retrieved results for the effective index of refraction, n, without and with gain for different pumping rates. The Re(μ) becomes more negative after the gain is introduced and the Im(μ) also drops significantly near the resonance. At a wavelength, $\lambda = 712$ nm, slightly higher than the resonance wavelength, the Re(n) reduces from -1.19 to -1.40 with a pumping rate, $\Gamma_{\text{pump}} = 1.6 \times 10^8\ \text{s}^{-1}$, and the Im($n$) drops from 0.83 to 0.26. Comparing these two Im(n), we can find the effective extinction coefficient $\alpha = (\omega/c)\text{Im}(n) \approx 7.35 \times 10^4\ \text{cm}^{-1}$ without gain and $\alpha \approx 2.3 \times 10^4\ \text{cm}^{-1}$ with a pumping rate of $1.6 \times 10^8\ \text{s}^{-1}$. Hence, we can obtain an effective amplification coefficient of $\alpha \approx -5.05 \times 10^4\ \text{cm}^{-1}$ for the combined system. This is much larger (on the order of 20) than the expected amplification of $\alpha \approx -2.5 \times 10^3\ \text{cm}^{-1}$ for the bulk gain at the pumping rate $\Gamma_{\text{pump}} = 1.6 \times 10^8\ \text{s}^{-1}$ [32]. This difference can be explained by the strong local-field enhancement inside the fishnet structure. In Fig. 3(c), we plot the figure-of-merit, FOM = $|\ \text{Re}(n)/\text{Im}(n)\ |$, versus the wavelength for different pumping rates. We find the FOM can reach a large value on the order of 100 in a certain wavelength range with the introduction of gain. It shows the gain compensates the losses of the fishnet metamaterial in this range.

4. Conclusions

We have numerically solved a self-consistent model incorporating gain into a 3D optical fishnet structure. We find the gain can compensate the losses of the optical fishnet metamaterial. The transmission, T, reflection, R, and absorption A with and without gain are presented for different pumping rates. As the pumping rate increases, both T and R clearly show a resonant behavior, and the absorption peak gets narrower since the gain undamps the magnetic resonance. We have also retrieved the effective parameters without gain and with gain for different pumping rates. Results show the losses are compensated with gain. From the retrieved index of refraction, n, the effective amplification of the combined system and the figure-of-merit, FOM, are calculated. The FOM increases dramatically with the pumping rate and the effective amplification coefficient is much larger than its bulk gain counterpart due to the strong local-field enhancement inside the fishnet structure.

In order to use the metamaterials in potential applications, one needs to reduce the losses at optical wavelengths. Although optical pumping can compensate losses as shown in this publication, it will not materialize real-world applications. In the future, for reducing losses with realistic applications, one needs to use semiconductors with gain (quantum dots or quantum wells), which can be pumped by electrical injection. This is compatible with the semiconductor industry. Although it is a difficult task, the metamaterial community will resolve this issue soon.

Acknowledgements

Work at Ames Laboratory was supported by the Department of Energy (Basic Energy Sciences) under Contract No. DE-AC02-07CH11358. This work was partially supported by the European Community FET project PHOME (Contract No. 213390) and by Laboratory-Directed Research and Development Program at Sandia National Laboratories. The author Z. Huang gratefully acknowledges support of the National Natural Science Foundation of China (Grant No. 60931002).

References

[1] J.B. Pendry, Contemp. Phys. 45 (2004) 191.
[2] S.A. Ramakrishna, Rep. Prog. Phys. 68 (2005) 449.

[3] C.M. Soukoulis, M. Kafesaki, E.N. Economou, Adv. Mater. 18 (2006) 1941.
[4] V.M. Shalaev, Nat. Photon. 1 (2007) 41.
[5] C.M. Soukoulis, S. Linden, M. Wegener, Science 315 (2007) 47.
[6] C.M. Soukoulis, M. Wegener, Science 330 (2010) 1633.
[7] F. Capolino, Theory and Phenomena of Metamaterials, CRC Press, Taylor and Francis Group, Boca Raton, FL, 2009.
[8] J.B. Pendry, Phys. Rev. Lett. 85 (2000) 3966.
[9] D. Schurig, et al. Science 314 (2006) 977.
[10] J. Zhou, Th. Koschny, C.M. Soukoulis, Opt. Express 16 (2008) 11147.
[11] J. Valentine, et al. Nature 455 (2008) 376.
[12] J. Zhou, et al. Phys. Rev. B 80 (2009) 035109.
[13] D.O. Guney, Th. Koschny, C.M. Soukoulis, Phys. Rev. B 80 (2009) 125129.
[14] S.A. Ramakrishna, J.B. Pendry, Phys. Rev. B 67 (2003) 201101.
[15] N.M. Lawandy, Appl. Phys. Lett. 85 (2004) 5040.
[16] M.A. Noginov, et al. Opt. Lett. 31 (2006) 3022.
[17] T.A. Klar, IEEE J. Sel. Top. Quantum Electron. 12 (2006) 1106.
[18] A.K. Sarychev, G. Tartakovsky, Phys. Rev. B 75 (2007) 085436.
[19] Y. Sivan, et al. Opt. Express 17 (2009) 24060.
[20] A.D. Boardman, et al. J. Opt. Soc. Am. B 24 (2007) A53.
[21] M. Wegener, et al. Opt. Express 16 (2008) 19785.
[22] A. Fang, Th. Koschny, M. Wegener, C.M. Soukoulis, Phys. Rev. B 79 (2009) 241104.
[23] A. Fang, Th. Koschny, C.M. Soukoulis, J. Opt. 12 (2010) 024013.
[24] A. Fang, Th. Koschny, C.M. Soukoulis, Phys. Rev. B 82 (2010) 121102.
[25] S. Wuestner, A. Pusch, K.L. Tsakmakidis, J.M. Hamm, O. Hess, Phys. Rev. Lett. 105 (2010) 127401.
[26] N.I. Zheludev, S.L. Prosvirnin, N. Papasimakis, V.A. Fedotov, Nat. Photon. 2 (2008) 351.
[27] D.J. Bergman, M.I. Stockman, Phys. Rev. Lett. 90 (2003) 027402.
[28] M.I. Stockman, Nat. Photon. 2 (2008) 327.
[29] K. Tanaka, E. Plum, J.Y. Ou, T. Uchino, N.I. Zheludev, Phys. Rev. Lett. 105 (2010) 227403.
[30] N. Meinzer, et al. Opt. Express 18 (2010) 24140.
[31] S. Xiao, et al. Nature 466 (2010) 735.
[32] A.E. Siegman, Lasers, Hill Valley, California, 1986, Chapters 2, 3, 6, and 13.
[33] P. Sperber, W. Spangler, B. Meier, A. Penzkofer, Opt. Quantum Electron. 20 (1988) 395.
[34] A. Taflove, Computational Electrodynamics: The Finite Difference Time Domain Method, Artech House, London, 1995, See Chapters 3, 6, and 7.
[35] D.R. Smith, S. Schultz, P. Markoŝ, C.M. Soukoulis, Phys. Rev. B 65 (2002) 195104.
[36] Th. Koschny, P. Markoŝ, E.N. Economou, D.R. Smith, D.C. Vier, C.M. Soukoulis, Phys. Rev. B 71 (2005) 245105.